FTIR Detection of Structural Changes in a Histidine Ligand during S-State Cycling of Photosynthetic Oxygen-Evolving Complex†

Yukihiro Kimura,*,‡ Naoki Mizusawa,§ Asako Ishii,⊥ and Taka-aki Ono*,‡

Laboratory for Photo-Biology (1), RIKEN Photodynamics Research Center, The Institute of Physical and Chemical Research, 519-1399 Aoba, Aramaki, Aoba, Sendai 980-0845, Japan

Received July 8, 2005; Revised Manuscript Received October 3, 2005

ABSTRACT: Changes in structural coupling between the Mn cluster and a putative histidine ligand during the S-state cycling of the oxygen-evolving complex (OEC) have been detected directly by Fourier transform infrared (FTIR) spectroscopy in photosystem (PS) II core particles from the cyanobacterium *Synechocystis* sp. PCC6803, in which histidine residues were selectively labeled with L-[$^{15}N_3$]histidine. The bands sensitive to the histidine-specific isotope labeling appeared at 1120−1090 cm^{-1} in the spectra induced upon the first-, second-, and fourth-flash illumination, for the S_2/S_1, S_3/S_2, and S_1/S_0 differences, at similar frequencies with different sign and/or intensity depending on the respective S-state transitions. However, no distinctive band was observed in the third-flash induced spectrum for the S_0/S_3 difference. The results indicate that a single histidine residue coupled with the structural changes of the OEC during the S-state cycling is responsible for the observed histidine bands, in which the histidine modes changed during the S_0-to-S_1 transition are reversed upon the S_1-to-S_2 and S_2-to-S_3 transitions. The 1186(+)/1178(−) cm^{-1} bands affected by L-[$^{15}N_3$]histidine labeling were observed only for the S_2/S_1 difference, but those affected by universal ^{15}N labeling appeared prominently showing a clear S-state dependency. Possible origins of these bands and changes in the histidine modes during the S-state cycling are discussed.

Photosynthetic water oxidation takes place in the oxygen-evolving complex (OEC),[1] which involves a catalytic metal center (Mn cluster) containing four Mn ions and one associated Ca ion located on the lumenal side of the photosystem (PS) II. The OEC catalyzes the oxidation of two water molecules to one oxygen molecule through a light-driven reaction cycle with five intermediate states denoted S_n ($n = 0-4$), where n represents the number of oxidizing equivalents stored. The cycle starts from the lowest oxidation state, S_0, and advances to higher S-states in a stepwise fashion by absorbing a photon. The OEC attains the highest oxidation state, S_4, by accumulating four oxidizing equivalents, and then spontaneously relaxes to the S_0-state concurrent with the release of an oxygen molecule (*1*). Since the dark-adapted OEC predominantly populates in a thermally stable S_1-state, oxygen evolves after the third flash.

The Mn cluster has been assembled and stabilized by several amino acid ligands mostly from the D1 protein (reviewed in refs *2* and *3*). The following amino acid residues of the D1 protein have been proposed to participate in ligation of the Mn cluster based on site-directed mutagenesis studies: carboxylate side chains from the Asp170, Glu189, Glu333, Asp342, and Ala344 and histidine side chains from His190, His332, and His337 (*2*−*9*). Asp170, Glu189, His332, and Glu333 have been reported to be direct ligands for the cluster in recent X-ray crystallographic models (*10*−*13*), although the interpretation of the electron density maps includes ambiguity in the location of the amino acid side chains (*13*). Spectroscopic evidence of the ligation in the Mn cluster has been provided in several amino acid residues in the D1 protein in combination with site-directed mutagenesis and/or isotope labeling. The D1-Asp170His mutants were largely normal in the S_1 and S_2 multiline EPR signals (*14*) and mid-frequency FTIR difference spectra during the S-state transitions (*15*), and therefore the D1-Asp170 carboxylate was assumed to ligate the Mn ion that involves no redox change during the S-state cycling (*15*). Isotope-edited FTIR studies on the C-terminal α-carboxylate of D1-Ala344 demonstrated ligation of the D1-Ala344 carboxylate from the redox-active Mn ion that is oxidized during the S_1-to-S_2 transition (*16*, *17*) and rereduced during the S_3-to-S_0 transition (*17*). In contrast, D1-Glu189 has been suggested to participate in a network of hydrogen bonds that modulates the properties of the Mn cluster and Y_Z tyrosine but is less likely as a direct ligand for the Mn cluster (*18*, *19*).

† This work was supported by grants from the Frontier Research System and Special Postdoctoral Researchers Programs at RIKEN.

* To whom correspondence should be addressed: Tel: +81 (48) 467 9547. Fax: +81 (48) 467 4679. E-mail: ykimura@riken.jp, takaaki@riken.jp.

‡ Present address: Molecular Membrane Biology Laboratory, RIKEN Discovery Research Institute, The Institute of Physical and Chemical Research, 2-1 Hirosawa, Wako 31-0198, Japan.

§ Present address: Department of Life Sciences, Graduate School of Arts and Sciences, The University of Tokyo, Komaba, Tokyo 153-8902, Japan.

⊥ Present address: Department of Biomedical Engineering, Toin Human Science and Technology Center, Toin University of Yokohama, 1614 Kurogane-cho, Aoba-ku, Yokohama 225-8502, Japan.

[1] Abbreviations: OEC, oxygen-evolving complex; PS, photosystem; Chl, chlorophyll; Q_A, primary quinone acceptor; FTIR, Fourier transform infrared; EPR, electron paramagnetic resonance; ESE, electron spin−echo; ENDOR, electron nuclear double resonance; ESEEM, electron spin−echo envelope modulation; Mes, 2-morpholinoethanesulfonic acid.

10.1021/bi051306r CCC: $30.25
Published on Web 11/15/2005

ESEEM (*20*) and ENDOR (*21*) studies on the S_2-state EPR multiline signal in PS II preparations from *Thermosynechococcus elongatus* universally labeled with ^{15}N demonstrated that at least one nitrogen atom is involved in coordination of the S_2-state Mn cluster. Further ESEEM (*22*) studies provided evidence that the Mn ion is ligated by at least one histidine residue using cyanobacterium *Synechocystis* sp. PCC6803, which contained imidazole nitrogen atoms selectively labeled with ^{15}N. A light-induced FTIR difference spectrum for the S_1-to-S_2 transition in this sample showed a band affected by the histidine-specific isotope labeling. The appearance of the band was interpreted to mean that a Mn ion oxidizable upon the S_1-to-S_2 transition is coordinated by the Nτ site of the imidazole ring of a histidine residue (*23*). Most of the D1-His190 mutants produced no oxygen evolution with the exception of retention of 10−13% activity in the Arg and Lys mutants (*8*, *24*). The D1-His190 acting as a proton acceptor from oxidized Y_Z (D1-Tyr161) (*8*, *24*−*26*) or participating in the redox reactions related to the assembly of the Mn cluster (*27*) also was suggested. The D1-His337Arg, Gln, Phe, and Asn mutants grew photoautotrophically with 18−51% oxygen-evolving activity (*9*). The relatively normal phenotypes of the Arg and Gln mutants suggested ligation of the arginine or glutamine side group as a replacement for the imidazole group of D1-His337 (*3*, *7*, *9*). However, it was also proposed that the D1-His337 participates in a hydrogen-bond network to be coupled with the Mn cluster indirectly as a hydrogen-bond donor (*3*, *9*). None of the D1-His332 mutants grew photoautotrophically other than the His332Gln and His332Ser mutants which evolved oxygen at rates 3−15% of the control (*9*). The D1-His332Glu mutant showed no O_2-evolving activity and abnormal magnetic properties of the S_2-state OEC (*28*). Further ESEEM study for this mutant indicated the ligation of the histidine residue to the Mn cluster (*29*). Recent X-ray crystallographic models (*12*, *13*) showed that D1-His332 provides a direct ligand to the Mn ion, suggesting that D1-His332 could be the most plausible candidate for the histidine ligand of the Mn cluster detected by pulsed EPR (*20*−*22*) and FTIR (*23*) measurements.

A histidine residue fulfills critical functional and structural roles as a ligand in many metalloenzymes and has been proposed to participate in proton and/or electron-transfer reactions during water oxidation (*30*). In the present study, we report for the first time a complete set of FTIR difference spectra during four S-state transition steps of the OEC using PS II core particles from the cyanobacterium *Synechocystis* sp. PCC 6803 in which histidine residues were selectively labeled with L-[$^{15}N_3$]histidine. Bands of the histidine ligands detected by histidine-specific isotope labeling showed characteristic changes during the S-state cycling of the OEC. Results indicate changes in structural coupling between the histidine ligand and Mn cluster during photosynthetic water oxidation.

MATERIALS AND METHODS

Sample Materials. A spontaneous histidine-tolerant mutant was isolated from the cyanobacterium *Synechocystis* sp. PCC 6803 strain retaining a histidine-tag on the C-terminal of CP47 (*31*) by repeated plating and selection of a single colony on BG-11 agar plates supplemented with increasing concentrations of L-histidine (30−240 μM) as reported (*22*). The histidine-tolerant strain obtained was grown photoautotrophically in liquid BG-11 medium containing L-histidine (^{14}N-His) or L-[$^{15}N_3$]histidine (^{15}N-His) ($^{15}N_3$, 98% ^{15}N enrichment, Cambridge Isotope Laboratories Inc.) at 30 °C under 20−100 μmol of photons m^{-2} s^{-1} in an 8 L Clearboy (Nalgene). Incorporation of ^{15}N-His into thylakoid membranes was determined to be approximately 88% by liquid chromatography/mass spectrometry. Harvested cells were disrupted using a Bead-beater (Bio-Spec Products), and resulting thylakoid membranes were solubilized with 0.8% (w/v) *n*-dodecyl-β-D-maltoside. After centrifugation, the resulting supernatant was loaded onto a Ni-NTA column (Qiagen) for purification as described previously (*31*). The resulting PS II core particles were concentrated by ultrafiltration to approximately 2 mg of Chl/mL and stored in liquid N_2. The O_2-evolving activity of the PS II core particles was approximately 2200 μmol of O_2 (mg of Chl)$^{-1}$ h^{-1} at 25 °C using 4 mM potassium ferricyanide as an electron acceptor.

Sample Preparation for FTIR Measurements. For FTIR measurements, the sample medium was replaced with medium A (40 mM sucrose, 5 mM NaCl, 5 mM $CaCl_2$, and 10 mM Mes/NaOH, pH 6.0) using repeated ultrafiltration in the presence of 0.06% (w/v) *n*-dodecyl-β-D-maltoside, and the PS II core suspensions were concentrated to approximately 3 mg of Chl/mL. PS II core suspension (7−8 μL, 3 mg of Chl/mL) supplemented with sodium ferricyanide (1 μL, 100 mM stock) as an electron acceptor was deposited on a BaF_2 disk (20 mm diameter) and then partially dried under a nitrogen stream (4 °C). After placing an aliquot (1 μL) of 20% (v/v) glycerol/water solution adjacent to the sample for control of the water content (*32*, *33*), the sample on the disk was covered by another BaF_2 disk with a greased Teflon spacer. The absorbance of the PS II sample was 0.8−1.0 at 1657 cm^{-1} after dark-incubation for 1.5 h. Sample temperature was maintained at 0 °C (±0.03 °C) using a homemade cryostat and temperature controller (Chino, KP1000) (*31*).

FTIR Measurements. FTIR spectra were recorded on a Bruker IFS-66v/s spectrophotometer equipped with an MCT detector (EG&G Optoelectronics D316/6) (*31*). A custom-made CdTe band-pass filter (2000−350 cm^{-1}) was placed in front of the sample to block He−Ne laser beam leakage from the interferometer compartment. A custom-made Ge long-pass filter (≥6 μm) was placed behind the sample to obtain a high-quality spectrum and to protect the detector element from laser scattering at the sample excitation (*33*). Excitation flashes were provided by a frequency-doubled Nd^{3+}:YAG laser (Spectra Physics INDI-50, 532 nm, pulse width 6−7 ns) with a flash energy of ∼10 mJ/cm^2 at the sample surface. For measurements of the flash-induced FTIR difference spectrum of each S-state transition, a dark-adapted sample was preflashed to enrich the S_1 population and reduce the oxidized non-heme iron at the acceptor side of the PS II. After subsequent incubation for 5 min in the dark, the sample was subjected to four successive flashes at 10-s intervals, and single-beam spectra (20 scans) were collected at 4 cm^{-1} resolution before the first flash and after each subsequent flash. This sequence was repeated 5−10 times with a 30-min interval for the dark adaptation for each sample. The single-beam spectrum before each flash was subtracted from that after the flash to obtain the flash-induced

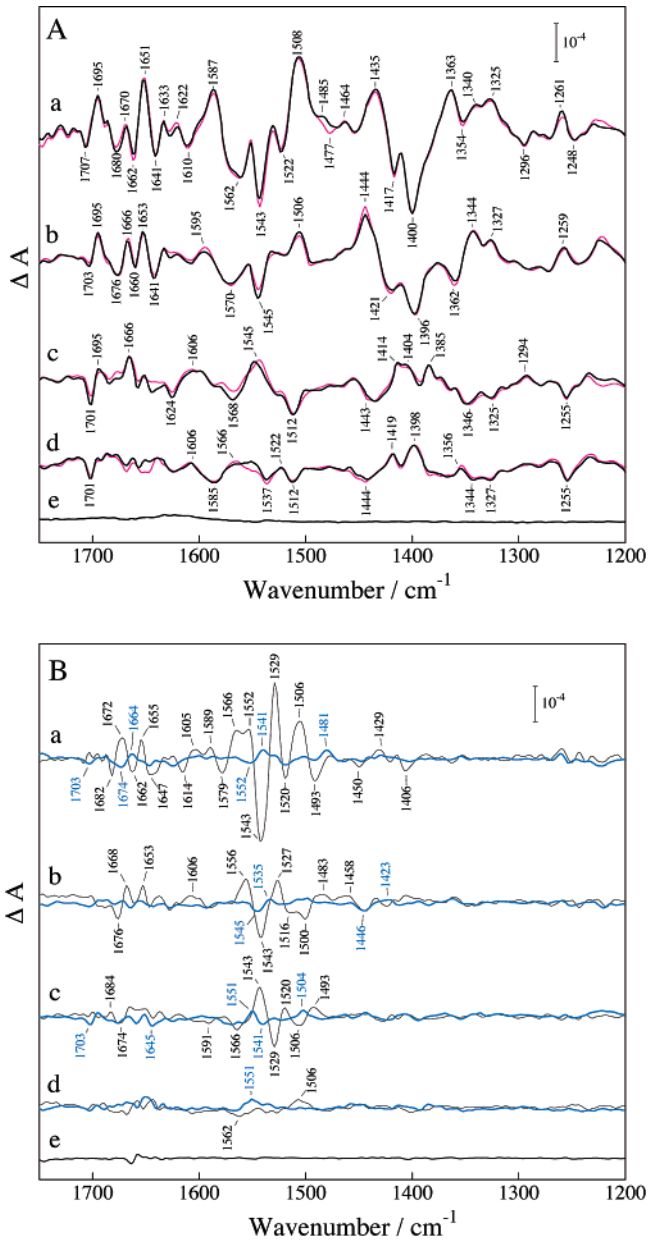

FIGURE 1: (A) Mid-frequency (1750−1200 cm^{-1}) FTIR difference spectra induced by the (a) first-, (b) second-, (c) third-, and (d) fourth-flash illumination of PS II core particles from unlabeled (black lines) and L-[$^{15}N_3$]histidine labeled (magenta lines) *Synechocystis* sp. PCC 6803 cells. A dark-minus-dark spectrum (e) is presented to show the noise level. (B) L-[$^{14}N_3$]Histidine/l-[$^{15}N_3$]-histidine double difference spectra (blue lines) for the differences upon the (a) first-, (b) second-, (c) third-, and (d) fourth-flash illumination, obtained by subtracting the L-[$^{15}N_3$]histidine labeled S-state difference spectra from the unlabeled S-state difference spectra after normalization with respect to peak intensity of symmetric carboxylate stretching bands (1450−1300 cm^{-1}). The universal $^{14}N/^{15}N$ double difference spectra (gray lines) for respective S-state transitions were calculated from the spectra in ref *33*. Spectrum e was presented to show the noise level for the double subtraction.

FTIR difference spectrum for each S-state transition. To improve the signal-to-noise ratio, 82−89 difference spectra (1640−1780 scans) were averaged.

RESULTS

Figure 1A shows the mid-frequency (1750−1200 cm^{-1}) FTIR difference spectra induced by the (a) first-, (b) second-, (c) third-, and (d) fourth-flash illumination of PS II core particles from unlabeled control (black lines) and ^{15}N-His labeled (magenta lines) *Synechocystis* sp. PCC 6803 cells of the histidine-tolerant strain. The unlabeled spectra upon the first- to fourth-flash illumination showed characteristic vibrational features mainly composed of amide I (1700−1600 cm^{-1}) and II (1600−1500 cm^{-1}) modes from the polypeptide backbones as well as symmetric (1450−1300 cm^{-1}) and asymmetric (1600−1500 cm^{-1}) stretching modes from the putative carboxylate ligands for the Mn cluster as reported previously (*15*, *17*, *32*−*34*). Apparent miss-hit factor for the S-state cycling was estimated to be approximately 18% from the oscillation pattern of several bands in the symmetric carboxylate stretching region (*33*). The spectra induced by the first-, second-, third-, and fourth-flash are thought to be contributed by the spectra for the S_2/S_1 (100%), S_3/S_2 (82%), S_0/S_3 (67%), and S_1/S_0 (55%) difference, respectively, and can be also referred to as the S_2/S_1, S_3/S_2, S_0/S_3, and S_1/S_0 difference spectra. ^{15}N-His labeling of two imidazole nitrogen atoms and one peptide nitrogen atom in histidine residues, minimally affected the S-state dependent vibrational features as shown in Figure 1A. However, some small but distinctive differences in peak positions and band intensities compared to those of unlabeled control spectra were observed.

The difference induced by ^{15}N-His labeling can be seen clearly in the ^{14}N-His/^{15}N-His double difference spectra (Figure 1B, blue lines) obtained by subtracting the ^{15}N-His labeled spectra from the unlabeled spectra for the respective S-state transitions after normalization with respect to the intensity of symmetric carboxylate stretching bands, which are insensitive to universal ^{15}N labeling (*33*, *34*). Figure 1B also shows the ^{14}N-U/^{15}N-U double difference spectra (gray lines), induced by universal ^{15}N labeling (*33*), plotted after normalization as a reference. Several bands in the ^{14}N-His/^{15}N-His double difference were observed in the amide I (1700−1600 cm^{-1}) and amide II (1600−1500 cm^{-1}) regions and appeared to change in sign and intensity during S-state transitions. Since amide I or II bands are ascribed to CO stretching modes slightly coupled with NH bending modes or CN stretching and NH bending modes of polypeptide backbones (*33*, *34*), the structural change in the polypeptide backbone moiety including the histidine nitrogen is a likely cause of the bands observed. However, band amplitudes were significantly smaller in the ^{14}N-His/^{15}N-His than in the ^{14}N-U/^{15}N-U double difference spectra, and band positions were markedly different between the two spectra. The ^{14}N-U/^{15}N-U double difference spectrum for the S_1/S_0 difference revealed the bands which have intensities that are considerably smaller than those for the S_2/S_1, S_3/S_2, and S_0/S_3 differences. This contrasts with comparable appearance of the ^{14}N-His/^{15}N-His bands during the S-state cycling. Notably, contribution from Q_A^-/Q_A bands to the present S_2/S_1 difference (first-flash) spectra for the unlabeled and ^{15}N-His labeled OECs can be excluded because of the absence of a prominent CO stretching band at 1478 cm^{-1} from Q_A^- (*35*). Therefore, structural changes in the polypeptide moiety including histidine residues may be responsible for the ^{15}N-His sensitive amide I and II bands during the S-state cycling.

Figure 2 shows the effects of ^{15}N-His labeling (A, magenta lines) and ^{15}N-U labeling (B, light-blue lines) on the mid-

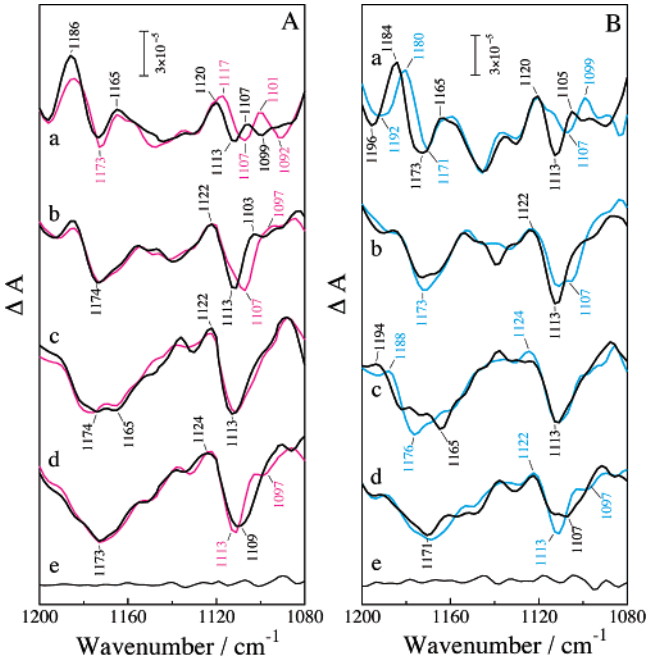

FIGURE 2: Effects of L-[$^{15}N_3$]histidine labeling (A, magenta lines) and universal ^{15}N labeling (B, light-blue lines) on FTIR difference spectra (1200−1080 cm^{-1}) upon the (a) first-, (b) second-, (c) third-, and (d) fourth-flash illumination of PS II core particles from unlabeled (black lines) and isotope labeled *Synechocystis* sp. PCC 6803 cells. The spectra presented in panel B were reproduced from ref *33*. Dark-minus-dark spectra (e) are presented to show the noise level.

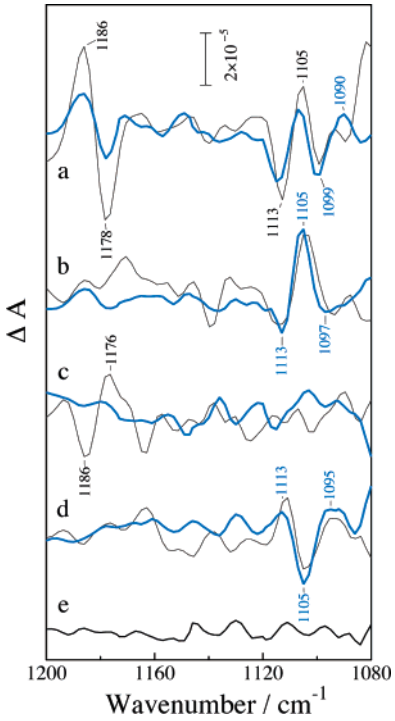

FIGURE 3: L-[$^{14}N_3$]Histidine/L-[$^{15}N_3$]histidine (blue lines) and universal $^{14}N/^{15}N$ (gray lines) double difference spectra for the differences upon the (a) first-, (b) second-, (c) third-, and (d) fourth-flash illumination. The double difference spectra were obtained by subtracting the isotope labeled S-state difference spectra from the unlabeled S-state difference spectra shown in Figure 2 after normalization with respect to peak intensity of symmetric carboxylate stretching bands (1450−1300 cm^{-1}). Spectrum e was presented to show the noise level for the double subtraction.

frequency (1200−1080 cm^{-1}) FTIR difference spectra[2] induced by the (a) first-, (b) second-, (c) third-, and (d) fourth-flash illumination of PS II core particles from *Synechocystis* sp. PCC 6803 cells. Unlabeled spectra induced upon the first- to fourth-flash illumination of the histidine-tolerant *Synechocystis* (A, black lines) showed characteristic vibrational features and S-state dependent changes that were similar to those of the wild-type *Synechocystis* (B, black lines), despite considerable overlaps of buffer bands and different contributions of the acceptor-side histidine band (*33*). The 1113(−) cm^{-1} band in the first-flash (S_2/S_1) spectrum was ascribed to the CN stretching mode of the histidine imidazole ring ligating the Mn cluster (*23*). A small band at 1099(−) cm^{-1} may be ascribed to the mode of histidine due to the reduction of the oxidized non-heme iron (Fe^{3+}) at the acceptor side (*23*, *36*, *37*). This assignment is compatible with the finding that this band intensified when the spectrum was measured without preflash (data not shown). The intensity of the non-heme iron band was relatively higher in the histidine-tolerant strain than in the wild-type strain. However, the intensity was much smaller than that reported in the previous study (*23*), in which the non-heme iron band less than 20% of the full population was induced.

The ^{15}N-His labeled spectra (magenta) possessed similar vibrational features as the unlabeled spectra for each S-state transition. However, the bands distinctively affected by ^{15}N-His labeling can be assigned to histidine residue(s) coupled to the Mn cluster. Upon ^{15}N-His labeling of the OEC, the 1120−1099 cm^{-1} bands in the first-flash (S_2/S_1) spectrum downshifted by 6−7 cm^{-1} in compatible with the extent of the downshift upon ^{15}N labeling for the CN stretching bands of the histidine residue ligating the metal center (*37*−*39*). The 1113(−)/1107(+) cm^{-1} and 1113(−)/1103(+) cm^{-1} bands in the first-flash (S_2/S_1) and second-flash (S_3/S_2) spectra seemed to downshift to 1107(−)/1101(+) cm^{-1} and 1107(−)/1097(+) cm^{-1}, respectively, in the ^{15}N-His labeled spectra. The effects of ^{15}N-His labeling also can be seen in the fourth-flash (S_1/S_0) spectra where a portion of the band at ∼1109 cm^{-1} was downshifted to 1097 cm^{-1} leaving the 1113(−) cm^{-1} buffer band (*33*). However, the third-flash (S_0/S_3) spectrum was minimally affected by ^{15}N-His labeling. As shown in panel B, ^{15}N-U labeling affected more bands at the 1200−1120 cm^{-1} range which was not much influenced by ^{15}N-His labeling, while both labelings similarly affected the bands at 1120−1090 cm^{-1}.

As shown in Figure 3, the $^{14}N/^{15}N$ isotopic bands can be seen clearly in the ^{14}N-His/^{15}N-His (blue lines) and ^{14}N-U/^{15}N-U (gray lines) double difference spectra obtained by subtracting the labeled spectrum from the unlabeled spectrum for each S-state transition shown in Figure 2. The ^{14}N-His/^{15}N-His double difference spectra coincided with the ^{14}N-U/^{15}N-U double difference spectra at 1120−1090 cm^{-1}, indicating that most of the bands influenced by universal ^{15}N labeling in this region can be predominantly ascribed to histidine residues. The ^{14}N-His/^{15}N-His double difference spectra for the S_2/S_1 difference contained bands at 1113(−)/1105(+)/1099(−)/1090(+) cm^{-1}. The first two

[2] The detectable limitation in the low-frequency region was 1080 cm^{-1} because of a much reduced signal-to-noise ratio of the spectrum lower than 1080 cm^{-1} due to the large absorption by water and buffer molecules.

bands and a large part of the 1099 cm^{-1} band may result from a downshift of the histidine bands at 1113(−)/1107(+) cm^{-1} to 1107(−)/1101(+) cm^{-1} upon ^{15}N-His labeling. The 1099(−)/1090(+) cm^{-1} double difference bands may partly include the acceptor side non-heme iron band that was downshifted from 1099(−) to 1092(−) cm^{-1} by the labeling (Figure 2A), but this contribution seemed to be small because the 1099(−) cm^{-1} band was similarly induced in the ^{14}N-U/^{15}N-U double difference spectrum for the S_2/S_1 difference, of which non-heme iron band was negligibly small as shown in Figure 2B. Therefore, it is reasonable to consider that the 1099(−) cm^{-1} double difference band is mainly caused by the isotopic downshift of the histidine band from 1107(+) to 1101(+) cm^{-1}, despite a small contribution of the non-heme iron band to the 1090(+) cm^{-1} double difference band.

DISCUSSION

The present results clearly demonstrate that the bands sensitive to ^{15}N-His labeling show distinct S-state dependency. The results provide the first evidence that a histidine residue is coupled to the structural changes of the OEC during the S-state cycling and are compatible with the view that a histidine residue provides a direct ligand to the Mn cluster. Therefore, these bands are attributable to the S-state dependent structural changes of the histidine ligand to the Mn cluster.

As shown in Figure 3, the ^{14}N-His/^{15}N-His double difference bands at 1113/1105/1099 cm^{-1} for the S_2/S_1 difference were also evident at almost the same frequencies in the double difference spectra for the S_3/S_2 and S_1/S_0 differences showing changes in their sign and intensity depending on the respective S-state transitions. In contrast, the S_0/S_3 spectrum did not show any clear ^{14}N-His/^{15}N-His double difference bands. These results indicate that the same histidine residue is responsible for these bands during the S-state cycling. X-ray crystallographic models of PS II at 3.2 and 3.5 Å indicated that D1-His332 acted as a direct ligand for the Mn ion, which is also coordinated by the carboxylate side group of D1-Glu189 (*12*, *13*). The 3.5 Å model further indicated that D1-His337 was not a direct ligand for the Mn cluster but could interact with one of the oxygen atoms in the cubane-like cluster core through hydrogen bonding (*12*). Therefore, these two residues can be potent candidates of the histidine residue responsible for the detected FTIR bands. However, the 1113(−) and 1107(+) cm^{-1} histidine bands for the S_2/S_1 difference were insensitive to H/D isotope exchange (*23*), and the histidine-manganese coupling detected by ESEEM showed no pH dependence in the range of pH 4.2−9.5 (*40*). These results indicate that D1-His332 is a preferable residue responsible for the observed histidine bands during the S-state cycling.

There are two possible interpretations for the absence of the histidine bands in the third-flash spectrum: (1) No structural change of the histidine residue upon the S_3-to-S_0 transition, (2) S_0/S_3 histidine bands exist but are concealed by the overlaps with the S_2/S_1 and S_3/S_2 histidine bands carried over. In the latter case, the third-flash spectrum can be composed of 67% S_0/S_3 signals, and 33% S_3/S_2 and S_2/S_1 signals by considering 18% miss-hit for the S-state transition, in which miss-hit OECs do not contribute to the light-induced FTIR difference spectra. If the histidine bands for the S_0/S_3 difference reflected the changes that canceled those upon the S_1-to-S_2 and S_2-to-S_3 transitions, the assumed S_0/S_3 histidine bands (67%) would be hard to conceal by 33% S_2/S_1 and S_3/S_2 histidine bands in the third-flash spectrum to appear as distinct bands with signs opposite to those for the S_2/S_1 and S_3/S_2 bands. Therefore, the first possibility is a preferable scenario, although the second possibility cannot be excluded completely.

As the fourth-flash spectrum includes 55% S_1/S_0 signals, and 45% S_0/S_3 and S_3/S_2 signals, it is reasonable to consider that the pure double difference spectrum for the S_1/S_0 difference would contain much intense 1105(−) cm^{-1} band and distinct 1113(+)/1095(+) cm^{-1} bands. If this is the case, the observed S-state dependence of the double difference spectra may be interpreted as the spectral changes of a single histidine residue ligating the Mn cluster, that is, the histidine bands at 1113(+)/1105(−)/1095(+) cm^{-1} that occur upon the S_0-to-S_1 transition were reversed upon the S_1-to-S_2 and S_2-to-S_3 transitions as revealed by the appearance of the 1113(−)/1105(+)/1099(−) cm^{-1} bands in the first-flash (S_2/S_1) spectrum and the 1113(−)/1105(+)/1097(−) cm^{-1} bands in the second-flash (S_3/S_2) spectrum. The Mn cluster is considered to be oxidized upon the S_0-to-S_1 and S_1-to-S_2 transitions but may not be oxidized upon the S_2-to-S_3 transition (*41*−*44*). Therefore, the observed changes of the histidine bands during the S-state cycling cannot be a simple reflection of the change in oxidation state of the Mn cluster but may include a large contribution from the structural changes of the OEC.

FTIR measurements along with L-[1-^{13}C]alanine labeling (*16*, *17*, *45*) and site-directed mutagenesis of D1-Ala344 (*46*, *47*) strongly indicate that the C-terminal α-carboxylate of the D1 protein ligates the Mn ion oxidized upon the S_1-to-S_2 transition and re-reduced upon the S_3-to-S_0 transition (*17*). Recent X-ray models suggested that D1-His332 ligates the Mn ion which is not directly associated with D1-Ala344 (*12*, 13). These results indicate that D1-His332 ligates the Mn ion which is different from the oxidizable Mn ion directly coupled to D1-Ala344. Therefore, the histidine bands for the S_2/S_1 difference are not likely to arise from the change of the D1-His332 mode directly induced by the oxidation of the coordinating Mn ion. This view is consistent with no appearance of the histidine bands in the S_0/S_3 (third-flash) spectrum, which may be accompanied by the reduction of the Mn ion ligated by the C-terminal α-carboxylate (*17*). Since resonant inelastic X-ray scattering studies indicated that electron transfer during the S_1-to-S_2 transition occurs from a delocalized orbital in the OEC (*48*), some change in electron density of the histidine-bound Mn ion may be responsible for the S_2/S_1 histidine bands in part. The Mn cluster core was suggested to undergo shrinking and expansion during the S_0-to-S_1 and S_2-to-S_3 transition as detected by changes in Mn−Mn distances using X-ray absorption spectroscopy (*43*, *44*, *49*). If the Mn−histidine interaction is affected by the structural shrinking and expansion of the Mn cluster core, the CN stretching bands of the histidine would be changed conversely by these changes and may contribute to the appearance of the 1105 cm^{-1} band with opposite sign in the fourth- and second-flash spectra for the S_1/S_0 and S_3/S_2 differences. At present, it is difficult to assign the corresponding histidine bands to respective S-states

definitively and to evaluate the details of the changes in the structure and/or oxidation state of the Mn cluster behind the observed spectral changes based on the double difference spectra. It is of note that D1-His332 is the primary candidate responsible for the observed histidine bands; we cannot exclude the possibility that a second histidine residue, which is structurally coupled with the Mn cluster, is responsible for some of the histidine bands.

The ^{14}N-His/^{15}N-His double difference spectra (Figure 3, blue lines) also showed mid-intensity bands at 1186(+) and 1178(−) cm^{-1} for the S_2/S_1 difference, although the bands did not show a clear S-state dependency. Previous reports assigned the 1179, 1109, 1102, 1090, and 1359 cm^{-1} bands in the Q_A^-/Q_A FTIR difference spectrum to side chain modes of the Q_A-coupled histidine (D2-His215) protonated at the Nπ site (*35*). However, the contribution of the Q_A^-/Q_A bands to the spectrum was negligibly small judging from the absence of other prominent ^{14}N-His/^{15}N-His double difference bands expected for the Q_A^-/Q_A difference (*35*). A possible vibrational candidate is NH deformation and CN stretching modes of the imidazole group of a histidine residue based on the DFT calculations (*50*) or CN stretching mode of the polypeptide main chain including the histidine residues (*51*). It is of note in this context that the ^{14}N-U/^{15}N-U double difference spectra for the S_2/S_1 difference (Figure 3, gray line) also showed much intense 1186(+)/1178(−) cm^{-1} bands. Corresponding inverse bands appeared at 1186(−)/1176(+) cm^{-1} in the double difference spectrum for the S_0/S_3 difference but were not observed for the S_3/S_2 and S_1/S_0 differences. Generally, the amide III (CN stretching and NH bending) mode of polypeptide backbones does not appear at frequencies lower than 1200 cm^{-1} (*52*). Therefore, the S-state dependent 1186/1178 cm^{-1} bands, sensitive to universal ^{15}N labeling but not sensitive to ^{15}N-His labeling, may be ascribed to the CN stretching mode of the polypeptide main chain coupled to the Mn cluster and/or a nitrogen-containing amino acid residue other than histidine. A possible candidate for the latter is the CN stretching vibrations of guanidinium group of an arginine side chain (*33*, *53*), which is structurally coupled to the Mn ion oxidized during the S_1-to-S_2 transition and reduced during the S_3-to-S_0 transition. It was reported that site-directed mutation of the Arg64 and Arg334 of D1 protein (*54*, *55*) or Arg305 and Arg342 of CP43 protein (*56*) influenced the OEC properties. Furthermore, a recent X-ray model indicated that the Arg357 side chain from CP43 protein is close to the active site of the Mn cluster (*12*), and participation of Arg357 in water oxidation for abstracting protons from a substrate water molecule was proposed (*57*). Therefore, structural changes of the guanidinium side chain of arginine may be responsible for the S-state dependent changes of ^{15}N-U sensitive but ^{15}N-His insensitive bands at 1186 and 1178 cm^{-1}.

REFERENCES

1. Debus, R. J. (1992) The manganese and calcium ions of photosynthetic oxygen evolution, *Biochim. Biophys. Acta 1102*, 269−352.
2. Diner, B. A. (2001) Amino acid residues involved in the coordination and assembly of the manganese cluster of photosystem II. Proton-coupled electron transport of the redox-active tyrosines and its relationship to water oxidation, *Biochim. Biophys. Acta 1503*, 147−163.
3. Debus, R. J. (2001) Amino acid residues that modulate the properties of tyrosine Y(Z) and the manganese cluster in the water oxidizing complex of photosystem II, *Biochim. Biophys. Acta 1503*, 164−186.
4. Nixon, P. J., and Diner, B. A. (1992) Aspartate 170 of the photosystem II reaction center polypeptide D1 is involved in the assembly of the oxygen-evolving manganese cluster, *Biochemistry 31*, 942−948.
5. Nixon, P. J., Trost, J. T., and Diner, B. A. **(**1992) Role of the carboxy terminus of polypeptide D1 in the assembly of a functional water-oxidizing manganese cluster in photosystem II of the cyanobacterium *Synechocystis* sp. PCC 6803: assembly requires a free carboxyl group at C-terminal position 344, *Biochemistry 31*, 10859−10871.
6. Chu, H.-A., Nguyen, A. P., and Debus, R. J. (1994) Site-directed photosystem II mutants with perturbed oxygen-evolving properties. 1. Instability or inefficient assembly of the manganese cluster in vivo, *Biochemistry 33*, 6137−6149.
7. Nixon, P. J., and Diner, B. A. (1994) Analysis of water-oxidation mutants constructed in the cyanobacterium *Synechocystis* sp. PCC 6803, *Biochem. Soc. Trans. 22*, 338−343.
8. Chu, H.-A., Nguyen, A. P., and Debus, R. J. (1995) Amino acid residues that influence the binding of manganese or calcium to photosystem II. 1. The lumenal interhelical domains of the D1 polypeptide, *Biochemistry 34*, 5839−5858.
9. Chu, H.-A., Nguyen, A. P., and Debus, R. J. (1995) Amino acid residues that influence the binding of manganese or calcium to photosystem II. 2. The carboxy-terminal domain of the D1 polypeptide, *Biochemistry 34*, 5859−5882.
10. Zouni, A., Witt, H.-T., Kern, J., Fromme, P., Krauss, N., Saenger, W., and Orth, P. (2001) Crystal structure of photosystem II from *Synechococcus elongatus* at 3.8 Å resolution, *Nature 409*, 739−743.
11. Kamiya, N., and Shen, J.-R. (2003) Crystal structure of oxygen-evolving photosystem II from *Thermosynechococcus vulcanus* at 3.7-Å resolution, *Proc. Natl. Acad. Sci. U.S.A. 100*, 98−103.
12. Ferreira, K. N., Iverson, T. M., Maghlaoui, K., Barber, J., and Iwata, S. (2004) Architecture of the photosynthetic oxygen-evolving center, *Science 303*, 1831−1837.
13. Biesiadka, J., Loll, B., Kern, J., Irrgang, K.-D., and Zouni, A. (2004) Crystal structure of cyanobacterial photosystem II at 3.2 Å resolution: a closer look at the Mn-cluster, *Phys. Chem. Chem. Phys. 6*, 4733−4736.
14. Debus, R. J., Aznar, C., Campbell, K. A., Gregor, W., Diner, B. A., and Britt, R. D. (2003) Does aspartate 170 of the D1 polypeptide ligate the manganese cluster in photosystem II? An EPR and ESEEM study, *Biochemistry 42*, 10600−10608.
15. Debus, R. J., Strickler, M. A., Walker, L. M., and Hillier, W. (2005) No evidence from FTIR difference spectroscopy that aspartate-170 of the D1 polypeptide ligates a manganese ion that undergoes oxidation during the S_0 to S_1, S_1 to S_2, or S_2 to S_3 transitions in photosytem II, *Biochemistry 44*, 1367−1374.
16. Chu, H.-A., Hiller, W., and Debus, R. J. (2004) Evidence that the C-terminus of the D1 polypeptide of photosystem II is ligated to the manganese ion that undergoes oxidation during the S_1 to S_2 transition: an isotope-edited study, *Biochemistry 43*, 3152−3166.
17. Kimura, Y., Mizusawa, N., Yamanari, T., Ishii, A., and Ono, T.-A. (2005) Structural changes of D1 C-terminal α-carboxylate during S-state cycling in photosynthetic oxygen evolution, *J. Biol. Chem. 280*, 2078−2083.
18. Debus, R. J., Cambell, K. A., Pham, D. P., Hays, A.-M. A., and Britt, R. D. (2000) Glutamate 189 of the D1 polypeptide modulates the magnetic and redox properties of the manganese cluster and tyrosine Y_Z in photosystem II, *Biochemistry 39*, 6275−6287.
19. Clausen J., Winkler, S., Hays, A.-M. A., Hundelt, M., Debus, R. J., and Junge, W. (2001) Photosynthetic water oxidation in *Synechocystis* sp. PCC6803: mutations D1-E189K, R and Q are without influence on electron transfer at the donor side of photosystem II, *Biochim. Biophys. Acta 1506*, 224−235.
20. DeRose, V. J., Yachandra, V. K., McDermott, A. E., Britt, R. D., Sauer, K., and Klein, M. P. (1991) Nitrogen ligation to manganese in the photosynthetic oxygen-evolving complex: Continuous-wave and pulsed EPR studies of Photosystem II particles containing ^{14}N or ^{15}N, *Biochemistry 30*, 1335−1341.
21. Tang, X.-S., Sivaraja, M., and Dismukes, G. C. (1993) Protein and substrate coordination to the manganese cluster in the photosynthetic water oxidizing complex: ^{15}N and ^{1}H ENDOR spectroscopy of the S_2 state multiline signal in the thermophilic cyanobacterium *Synechococcus elongatus*, *J. Am. Chem. Soc. 115*, 2382−2389.

22. Tang, X.-S., Diner, B. A., Larsen, B. S., Gilchrist, M. L., Lorigan, G. A., and Britt, R. D. (1994) Identification of histidine at the catalytic site of the photosynthetic oxygen-complex, *Proc. Natl. Acad. Sci. U.S.A. 91*, 704−708.
23. Noguchi, T., Inoue, Y., and Tang, X.-S. (1999) Structure of a histidine ligand in the photosynthetic oxygen-evolving complex as studied by light-induced fourier transform infrared difference spectroscopy, *Biochemistry 38*, 10187−10195.
24. Hays, A.-M. A., Vassiliev, I. R., Golbeck, J. H., and Debus, R. J. (1998) Role of D1-His190 in proton-coupled electron-transfer reactions in photosystem II: A chemical complementation study, *Biochemistry 37*, 11352−11365.
25. Mamedov, F., Sayre, R. T., and Styring, S. (1998) Involvement of histidine 190 on the D1 protein in electron/proton-transfer reactions on the donor side of photosystem II, *Biochemistry 37*, 14245−14256.
26. Hays, A.-M. A., Vassiliev, I. R., Golbeck, J. H., and Debus, R. J. (1999) Role of D1-His190 in the proton-coupled oxidation of tyrosine Y_Z in manganese-depleted photosystem II, *Biochemistry 38*, 11851−11865.
27. Roffey, R. A., Kramer, D. M., Govindjee, Sayre, R. T. (1994) Lumenal side histidine mutations in the D1 protein of Photosystem II affect donor side electron transfer in *Chlamydomonas reinhardtii*, *Biochim. Biophys. Acta 1185*, 257−270.
28. Debus, R. J., Cambell, K. A., Peloquin, J. M., Pham, D. P., and Britt, R. D. (2000) Histidine 332 of the D1 polypeptide modulates the magnetic and redox properties of the manganese cluster and tyrosine Y_Z in photosystem II, *Biochemistry 39*, 470−478.
29. Debus, R. J., Cambell, K. A., Cregor, W., Li, Z.-L., Burnap, R. L., and Britt, R. D. (2001) Does histidine 332 of the D1 polypeptide ligate the manganese cluster in photosystem II? An electron spin−echo envelope modulation study, *Biochemistry 40*, 3690−3699.
30. Padhye, S., Kambara, T., Hendrickson, D. N., and Govindjee (1986) Manganese-histidine cluster as the functional center of the water oxidation complex in photosynthesis, *Photosynth. Res. 9*, 103−112.
31. Kimura, Y., Mizusawa, N., Ishii, A., Yamanari, T., and Ono, T.-A. (2003) Changes of low-frequency vibrational modes induced by universal ^{15}N- and ^{13}C-isotope labeling in S_2/S_1 FTIR difference spectrum of oxygen-evolving complex, *Biochemistry 42*, 13170−13177.
32. Noguchi, T., and Sugiura, M. (2002) Flash-induced FTIR difference spectra of the water oxidizing complex in moderately hydrated photosystem II core films: effect of hydration extent on S-state transitions, *Biochemistry 41*, 2322−2330.
33. Yamanari, T., Kimura, Y., Mizusawa, N., Ishii, A., and Ono, T.-A. (2004) Mid-to-low-frequency Fourier transform infrared spectra of S-state cycle for photosynthetic oxygen evolution in *Synechocystis* sp. PCC 6803, *Biochemistry 43*, 7479−7490.
34. Noguchi, T., and Sugiura, M. (2003) Analysis of flash-induced FTIR defference spectra of the S-state cycle in the photosynthetic water-oxidizing complex by uniform ^{15}N and ^{13}C isotope labeling, *Biochemistry 42*, 6035−6042.
35. Noguchi, T., Inoue, Y., and Tang, X.-S. (1999) Hydrogen bonding interaction between the primary quinone acceptor Q_A and a histidine side chain in photosystem II As revealed by Fourier transform infrared spectroscopy, *Biochemistry 38*, 399−403.
36. Noguchi, T., and Inoue, Y. (1995) Identification of Fourier transform infrared signals from the non-heme iron in photosystem II, *J. Biochem. 118*, 9−12.
37. Hienerwadel, R., and Berthomieu, C. (1995) Bicarbonate binding to the non-heme iron of photosystem II investigated by Fourier transform infrared difference spectroscopy and ^{13}C-labeled bicarbonate, *Biochemistry 34*, 16288−16297.
38. Breton, J., Xu, W., Diner, B. A., and Chitnis, P. R. (2002) The two histidine axial ligands of the primary electron donor chlorophylls (P700) in photosystem I are similarly perturbed upon $P700^+$ formation, *Biochemistry 41*, 11200−11210.
39. Dupeyrat, F., Vidaud, C., Lorphelin, A., and Berthomieu, C. B. (2004) Long distance charge redistribution upon Cu, Zn-superoxide dismutase reduction, *J. Biol. Chem. 279*, 48091−48101.
40. Gregor, W. G., and Britt, R. D. (2000) Nitrogen ligation to the manganese cluster of photosystem II in the absence of the extrinsic proteins and as a function of pH, *Photosynth. Res 65*, 175−185.
41. Ono, T.-A., Noguchi, T., Inoue, Y., Kusunoki, M., Matsushita, T., and Oyanagi, H. (1992) X-ray-detection of the period-4 cycling of the manganese cluster in photosynthetic water oxidizing enzyme, *Science 258*, 1335−1337.
42. Roelofs, T. A., Liang, W., Latimer, M. J., Cinco, R. M., Rompel, A., Andrews, J. C., Sauer, K., Yachandra, V. K., and Klein, M. P. (1996) Oxidation states of the manganese cluster during the flash-induced S-state cycle of the photosynthetic oxygen-evolving complex, *Proc. Natl. Acad. Sci. U.S.A. 93*, 3335−3340.
43. Liang, W., Roelofs, T. A., Cinco, R. M., Rompel, A., Latimer, M. J., Yu, W. O., Sauer, K., Klein, M. P., and Yachandra, V. K. (2000) Structural change of the Mn cluster during the $S_2 \rightarrow S_3$ state transition of the oxygen-evolving complex of photosystem II. Does it reflect the onset of water/substrate oxidation? Determination by Mn X-ray absorption spectroscopy, *J. Am. Chem. Soc. 122*, 3399−3412.
44. Messinger, J., Robblee, J. H., Bergmann, U., Fernandez, C., Glatzel, P., Visser, H., Cinco, R. M., McFarlane, K. L., Bellacchio, E., Pizarro, S. A., Cramer, S. P., Sauer, K., Klein, M. P., and Yachandra, V. K. (2001) Absence of Mn-centered oxidation in the $S_2 \rightarrow S_3$ transition: implications for the mechanism of photosynthetic water oxidation, *J. Am. Chem. Soc. 123*, 7804−7820.
45. Strickler, M. A., Walker, L. M., Hillier, W., and Debus, R. J. (2005) Evidence from biosynthetically incorporated strontium and FTIR difference spectroscopy that the C-terminus of the D1 polypeptide of photosystem II does not ligate calcium, *Biochemistry 44*, 8571−8577.
46. Mizusawa, N., Kimura, Y., Ishii, A., Yamanari, T., Nakazawa, S., Teramoto, H., and Ono, T.-A. (2004) Impact of replacement of D1 C-terminal alanine with glycine on structure and function of photosynthetic oxygen-evolving complex, *J. Biol. Chem. 279*, 29622−29627.
47. Mizusawa, N., Yamanari, T., Kimura, Y., Ishii, A., Nakazawa, S., and Ono, T.-A. (2004) Changes in the functional and structural properties of the Mn cluster induced by replacing the side group of the C-terminus of the D1 protein of photosystem II, *Biochemistry 43*, 14644−14652.
48. Glatzel, P., Bergmann, U., Yano, J., Visser, H., Robblee, J. H., Gu, W., de Groot, F. M. F., Christou, G., Pecoraro, V. L., Cramer, S. P., and Yachandra, V. K. (2004) The electronic structure of Mn in oxides, coordination complexes, and the oxygen-evolving complex of photosystem II studied by resonant inelastic X-ray scattering, *J. Am. Chem. Soc. 126*, 9946−9959.
49. Robblee, J. H., Messinger, J., Cinco, R. M., McFarlane, K. L., Fernandez, C., Pizarro, S. A., Sauer, K., and Yachandra, V. K. (2002) The Mn cluster in the S_0 state of the oxygen-evolving complex of photosystem II studied by EXAFS spectroscopy: Are there three di-μ-oxo-bridged Mn_2 moieties in the tetranuclear Mn complex? *J. Am. Chem. Soc. 124*, 7459−7471.
50. Hasegawa, K., Ono, T.-A., and Noguchi, T. (2002) Ab initio density functional theory calculations and vibrational analysis of zinc-bound 4-methylimidazole as a model of a histidine ligand in metalloenzymes, *J. Phys. Chem. A 106*, 3377−3390.
51. Krimm, S., and Bandekar, J. (1986) Vibrational spectroscopy and conformation of peptides, polypeptides, and proteins. *Adv. Protein Chem. 38*, 181−364.
52. Socrates, G. (1994) in *Infrared and Raman Characteristic Group Frequencies*, 3rd ed.; pp 333−335, John Wiley & Sons, Chichester.
53. Braiman, M. S., Briercheck, D. M., and Kriger, K. M. (1999) Modeling vibrational spectra of amino acid side chains in proteins: Effects of protonation state, counterion, and solvent on arginine C−N stretch frequencies, *J. Phys. Chem. B 103*, 4744−4750.
54. Li, Z.-L., and Burnap, R. L. (2001) Mutations of Arginine 64 within the Putative Ca^{2+}-Binding Lumenal Interhelical a−b Loop of the Photosystem II D1 Protein Disrupt Binding of the Manganese Stabilizing Protein and Cytochrome c_{550} in *Synechocystis* sp. PCC6803, *Biochemistry 40*, 10350−10359.
55. Li, Z., and Burnap, R. L. (2002) Mutations of basic arginine residue 334 in the D1 protein of Photosystem II lead to unusual S_2 state properties in *Synechocystis* sp. PCC 6803, *Photosynth. Res. 72*, 191−201.
56. Knoepfle, N., Bricker, T. M., and Putnam-Evans, C. (1999) Site-directed mutagenesis of basic arginine residue 305 and 342 in the CP 43 protein of photosystem II affects oxygen-evolving activity in *Synechocystis* 6803, *Biochemistry 38*, 1582−1588.
57. McEvoy, J. P., and Brudvig, G. W. (2004) Structure-based mechanism of photosynthetic water oxidation, *Phys. Chem. Chem. Phys. 6*, 4754−4763.

BI051306R